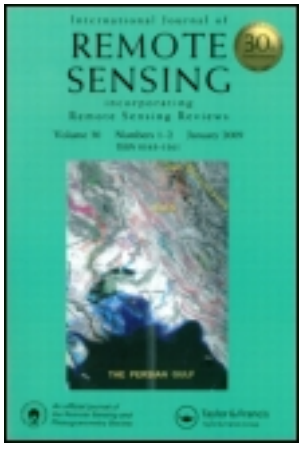

International Journal of Remote Sensing

Publication details, including instructions for authors and subscription information:
http://www.tandfonline.com/loi/tres20

A new approach for forest decline assessments: maximizing detail and accuracy with multispectral imagery

Jennifer Pontius[ab]

[a] Rubenstein School of Environment and Natural Resources, University of Vermont, Burlington, VT, USA

[b] USDA Forest Service, Northern Research Station, Burlington, VT 05405, USA

Published online: 17 Apr 2014.

To cite this article: Jennifer Pontius (2014) A new approach for forest decline assessments: maximizing detail and accuracy with multispectral imagery, International Journal of Remote Sensing, 35:9, 3384-3402, DOI: 10.1080/01431161.2014.903439

To link to this article: http://dx.doi.org/10.1080/01431161.2014.903439

International Journal of Remote Sensing, 2014
Vol. 35, No. 9, 3384–3402, http://dx.doi.org/10.1080/01431161.2014.903439

Taylor & Francis
Taylor & Francis Group

A new approach for forest decline assessments: maximizing detail and accuracy with multispectral imagery

Jennifer Pontius*

Rubenstein School of Environment and Natural Resources, University of Vermont, Burlington, VT, USA; USDA Forest Service, Northern Research Station, Burlington, VT 05405, USA

(*Received 27 June 2013; accepted 2 March 2014*)

Remote sensing of forest condition is typically based on broadband vegetation indices to quantify coarse categories of canopy condition. More detailed and accurate assessments have been demonstrated using narrowband sensors, although with more limited image availability. While differences in sensor capabilities are obvious, I hypothesized that multispectral imagery may be able to detect more subtle canopy stress symptoms if a new calibration approach was considered. This involves three major changes to traditional decline assessments: (1) calibration with more detailed field measurements, (2) consideration of narrowband derived indices adapted for broadband calculation, and (3) a multivariate calibration model. Testing this approach on Landsat-5 (TM) imagery in the Catskills, NY, USA, a five-term linear regression model (r^2 = 0.621, RMSE 0.403) based on a unique combination of vegetation indices sensitive to canopy chlorophyll, carotenoids, green leaf area, and water content was able to quantify a broad range of forest condition across species. When rounded to a class-based system for comparison to more traditional methods, this equation predicted decline across 42 mixed-species plots with 65% accuracy (10-classes), and 100% accuracy (5-classes). This approach was a significant improvement over commonly used vegetation indices such as NDVI (r^2 = 0.351, RMSE = 0.500, 10-class accuracy = 60%, and 5-class accuracy = 74%). These results suggest that relying solely on a single common vegetation index to assess forest condition may artificially limit the accuracy and detail possible with multispectral imagery. I recommend that future efforts to monitor forest decline consider this three-pronged approach to decline predictions in order to maximize the information and accuracy obtainable with broadband sensors so widely available at this time.

1. Introduction

Multispectral remote-sensing sensors such as Landsat have been used for decades to assess a suite of vegetation biophysical parameters. These studies often employ vegetation indices (VIs) based on the unique reflectance characteristics of vegetation across the visible and near infrared wavelengths. The most common include the ratio vegetation index (RVI) (Pearson and Miller 1972) and NDVI (Rouse et al. 1974). Noting the sensitivity of common indices to changes in background properties, another class of indices was designed to account for soil and atmospheric background variations (e.g. soil adjusted vegetation index (SAVI) – (Keane, Morgan, and Menakis 1994) transformed SAVI (TSAVI) (Arzani and King 1997)). In forest health applications, these indices are typically used to identify broad categories of forest condition (primarily characterized as defoliation classes) for a single species of interest. For example,

*Email: Jennifer.pontius@uvm.edu

Lambert et al. (1995) used Landsat imagery to separate three categories of damage in Norway spruce with 75% accuracy; Royle and Lathrop (2002) predicted four classes of hemlock defoliation with 82% accuracy; Wang, Lu, and Haithcoat (2007) quantified five categories of oak decline in response to the drought of 1999 with 76% accuracy; and Arsenault et al. (2006) separated aspen into light, moderate, and severe damage with 70% accuracy.

While this approach may be useful for assessing extreme changes in specific forest canopies, limiting decline predictions to a small number of coarse classes lacks the detail necessary to detect early, more subtle decline symptoms or monitor long-term trends over time. Addressing this limitation to categorical assessments of forest condition, Townsend et al. (2012) used Landsat to map continuous canopy defoliation, quantified as a change in common vegetation indices, between gypsy moth defoliation and non-defoliation years. Their final model was able to estimate defoliation, with RMSE = 14.9% and cross-validation $r^2 = 0.805$. While this represents an improvement over typical broad categorical assessments of forest condition, it still focuses on acute, severe stress events in relatively homogeneous deciduous stands.

In contrast to multispectral efforts, narrowband hyperspectral sensors have been used to quantify a range of forest biophysical, structural, and process-based (e.g. productivity) characteristics. The accuracy of these efforts can be attributed to both the narrow spectral signal of key biophysical absorbance features that can be detected with narrowband sensors and the analytical calculations possible with many contiguous bands. The development of narrowband indices is typically based on laboratory samples where wavelengths of known sensitivity to the target biophysical parameter (such as chlorophyll content, chlorophyll fluorescence, or leaf water content) are linked to a parameter 'insensitive' control band. This has resulted in the development of indices to quantify chlorophyll concentration (Gitelson and Merzlyak 1996), photosynthetic activity (Carter 1998; Carter, Cibula, and Miller 1996), and micronutrient content (Adams et al. 2000) to name a few. Hyperspectral sensors have also been used to quantify forest decline. Pontius, Hallett, and Martin (2005a) used NASA's AVIRIS sensor to predict hemlock woolly adelgid (*Adelges tsugae*)-induced decline in eastern hemlock (*Tsuga Canadensis*) and used SpecTIR's VNIR sensor to locate incipient emerald ash borer (*Agrilus planipennis*) infestations in various *Fraxinus* spp. (Pontius et al. 2008).

In an attempt to merge the information and detail available from hyperspectral imagery with the widespread availability of multispectral imagery, a forest decline assessment method is proposed that hinges on three novel components. First is the characterization of forest condition for image calibration using a detailed, continuous summary decline rating that captures a gradient of vegetation stress symptoms (Pontius and Hallett forthcoming). This is a departure from the broad classes of canopy condition typically used to assess forest decline.

Second is the consideration of a suite of vegetation indices, including narrowband-derived indices typically utilized only with hyperspectral sensors. Because these narrowband indices are based on the assumption that biophysical characteristics symptomatic of vegetation stress are characterized in narrow absorbance features, it is unlikely that a broadband sensor is able to quantify these specific parameters with the same precision as narrowband sensors. However, it is possible that calculating a broadband 'equivalent' of narrowband-derived indices (see Section 2.2) could capture unique characteristics of vegetation stress that may be useful in decline assessments.

The final component of the proposed approach involves the development of a multivariate predictive model that combines a suite of indices, with careful consideration of autocorrelation and model overfitting. In combination, I hypothesized that this three-

pronged approach can provide a more detailed and accurate assessment of forest condition than models based on traditional indices.

2. Methods

2.1. Field methods

This study builds on prior hyperspectral efforts (Pontius, Hallett, and Martin 2005a, 2005b) in the Catskill Mountains region of NY (Figure 1). The Catskills were selected based on the convergence of many forest stress agents, range of species composition, and elevational gradients. It is also a key source of water for the New York City metropolitan area, making the function and condition of its forested watersheds of prime interest. In 2007, forty-three forest-monitoring plots (Figure 1) were visited across the region spanning a range of forest condition, species, and site characteristics. This included plots dominated by maple (*Acer*), birch (*Betula*), pine (*Pinus*), hemlock (*Tsuga*), oak (*Quercus*), cherry (*Prunus*), and fir (*Abies*) species. Common stressors across the region include moisture availability, acid deposition and associated cation leaching, hemlock woolly adelgid, beech bark disease, and periodic forest tent caterpillar outbreaks.

To minimize misregistration error, plots were located in stands where topographic characteristics, species composition, and structure were consistent beyond the bounds of the plot. At each plot, a suite of decline characteristics was quantified for all canopy dominant trees counted as 'in' by a 10-factor prism. In order to capture early stress symptoms, along with more traditional, ocular assessments of canopy condition, I measured a suite of variables designed to capture a range of expected vegetation response to stress. This included measurements of chlorophyll fluorescence (performance index obtained using a Handy PEA chlorophyll fluorometer (http://www.nutechintl.com/hansatech-handy-pea.htm), percentage canopy transparency quantified using digital photographs of tree canopies

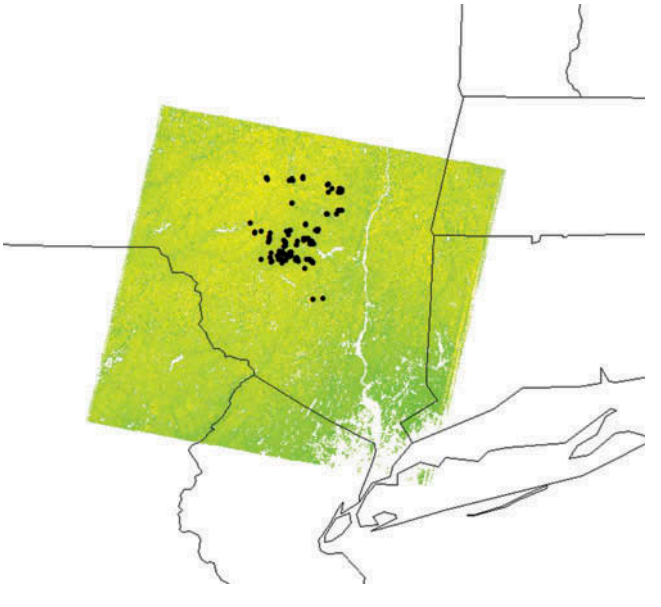

Figure 1. The Catskills region study area (~UTM WGS84 550000 E 4620000 N) included 42 plots selected to cover a range of species composition, stress agents, and decline severities.

taken in the field, percentage fine twig dieback, and percentage live crown and crown vigour class following Forest Health Monitoring guidelines (USDA 1997). Additional measures of percentage new growth were included for hemlock, while percentage defoliation was subjectively assessed into 10% increments for hardwoods.

In order to summarize information from each of these measurements into one continuous, summary decline rating, each variable was standardized to a 0–10 scale based on species-specific population distributions from over 10 years of field sampling across the northeastern USA (available from the author upon request). Using percentiles based on a minimum of 100 individuals and spanning a full range of possible tree conditions, from optimal health to dead, each decline variable was normalized and standardized by species. Percentile assignments for all measured decline symptoms were then averaged for each tree to produce a continuous summary decline rating for each tree. Plot-level condition for image calibration was calculated as the average of all trees weighted by species percentage basal area. This plot-level-weighted average percentile scores was multiplied by 10 to force a 0–10 decline scale. To exemplify this process, field measurements, standardized percentiles, and final decline rating calculations are presented in Table 1.

The resulting plot-level decline summary rating ranged from 2 to 5.97, with a mean of 4.02 and standard deviation of 0.68. Combining multiple stress characteristics into one summary decline rating provides a comprehensive, continuous measure for more detailed image calibration, from early reductions in photosynthetic function (chlorophyll fluorescence) to indicators of imminent death (live crown ratio) (Pontius and Hallett 2014).

2.2. Image processing

Landsat-5 (TM) has acquired images of the Earth nearly continuously since1982, with a 16-day repeat cycle, 185 km swath, and 30 m resolution. A mid-growing season (15 June–15 August) Landsat-5 (TM), level 1T image was downloaded from the USGS Global Visualization Viewer (http://glovis.usgs.gov/). Level 1T imagery includes orthorectification and radiometric correction using the revised calibration gains for the reflective bands 1–5 and 7 (Chander, Markham, and Helder 2009). In order to account for solar illumination angle, atmospheric path length, and differences in sensor characteristics (i.e. gain and bias), DN values were converted to top of the atmosphere (TOA) reflectance using ENVI 4.6.1's Landsat-5 (TM) calibration (ITT Visible Solutions, Inc.). I converted TOA reflectance to at-surface reflectance for vegetation index calculations using a dark object subtraction based on the lowest digital number that first reached 0.1% of all pixels in the image histogram (Chavez 1988; Soudani et al. 2006). This method has been shown to work as well or better than more complicated radiative transfer models at reducing the differences in surface reflectance estimation between multi-date images (Song et al. 2001). Multispectral data for bands 1–5 and 7 were extracted from the pixel whose centre was located closest to plot centre.

2.3. Model calibration and accuracy assessment

Vegetation indices considered in this study can be grouped into two broad categories, traditional and narrowband-derived indices. To test possible vegetation indices for assessments of forest condition, I include a suite of traditional broadband indices. To test the utility of narrowband-derived indices as well, I created a database that would calculate a Landsat-5 (TM) equivalent for a suite of narrowband indices known for their sensitivity to

Table 1. An example of the plot summary decline rating calculation for a plot with five canopy dominant trees representing three different species. Field-measured values (FMV) are first normalized to a species-based percentile score (SBP) based on a database of over 2000 trees from across the northeast. Percentiles for all variables are averaged for each tree and then by species so that a plot-level average can be weighted by species percentage basal area. This final weighted average percentile score is then multiplied by 10 for the 0–10 decline scale.

	Acer rubrum-1		*Acer rubrum-2*		*Acer saccharum-1*		*Fagus grandifolia-1*		*Fagus grandifolia-2*	
Field measurement	FMV	SBP	FMV	SBP	FMV	SBP	FMV	SBP	FMV	SBP
Crown vigour	1	0.21	2	0.60	1	0.24	1	0.23	1	0.23
Percentage dieback	5	0.28	10	0.55	5	0.36	5	0.29	5	0.29
FvFm	0.79	0.06	0.82	0.76	0.82	0.69	0.79	0.19	0.86	0.93
Percentage live crown	0.61	0.81	0.60	0.80	0.44	0.35	0.67	0.84	0.61	0.73
PI	1.99	0.05	2.84	0.19	2.17	0.12	1.52	0.10	2.60	0.17
Tree average	*0.28*		*0.58*		*0.35*		*0.33*		*0.47*	
Species average		*0.43*				*0.35*		*0.40*		
Percentage plot basal area		*0.55*				*0.15*		*0.30*		
Plot weighted average				*(0.43 × 0.55) + (0.35 × 0.15) + (0.40 × 0.30) = 0.41*						
Plot summary decline rating *0–10 scale*				0.14 × 10 = **4.1**						

vegetation stress characteristics. Equivalences were used for any index where the narrowband required for calculation was contained within the Landsat spectral range, and all variables required for index calculation fell within distinct bands. As an example where a Landsat equivalent could be calculated, consider the chlorophyll$_b$-sensitive index proposed by Datt (1998). This narrowband index is calculated as (R_{672} nm/R_{550} nm). Considering that Landsat-5 (TM) band 2 ranges from 520 to 600 nm and band 3 measures between 630 and 690 nm, I calculated a broadband equivalent to Datt's index as Landsat-5 (TM) (Band3/Band2).

While the expectation is that much of the specific information pertinent to chlorophyll$_b$ content captured in the narrowband equation will be lost in the broadband equivalent due to the narrow chlorophyll$_b$ absorption feature, there may still be enough information relative to vegetation stress condition to make it useful in a more complex, multivariate model. Final indices considered included 16 multispectral and 22 modified narrowband-derived stress-sensitive indices (Table 2).

Spearman's Rho non-parametric and partial correlations were used to quantify relationships between each individual vegetation index and the summary decline rating. All traditional broadband and narrowband derived indices, as well as reflectance for Landsat (TM) bands 1–5 and 7, were included in a mixed, stepwise linear regression. Final models were limited to a maximum of five terms (Williams and Norris 2001) and $\alpha < 0.05$ to avoid over-fitting. Various models were compared using the Akaike Information Criterion (AIC). This provides a measure of the tradeoff between bias and variance as the number of variables in a model grows (Akaike 1976). Because many of the indices selected were based on various combinations of the same Landsat-5 (TM) bands, it was essential to ensure that autocorrelation between predictor variables was minimized. Therefore, in addition to AIC model assessment, any variable with a variance inflation factor (VIF) greater than 4 was eliminated. Typically, autocorrelation is considered to be negligible when VIF is less than 10 (Kleinbaum et al. 1998). Jack-knifed residuals were also used to assess the stability of the final predictive equation as an estimate of accuracy on independent data (Kozak and Kozak 2003).

In order to compare this multivariate approach to traditional multispectral indices, simple linear regressions were also established for each of the individual indices and evaluated based on fit, significance, RMSE, and PRESS jack-knifed residuals (Kozak and Kozak 2003). In order to compare the accuracy of this multivariate approach to more common categorical assessments of forest condition, I also converted the continuous decline rating to a class variable by rounding to the nearest integer, and grouping predictions into a 10-class ranking for accuracy assessment.

3. Results and discussion

3.1. Univariate correlations

Spearman's non-parametric correlations identified a large number of both traditional and narrowband indices significantly correlated with the field summary decline rating (Table 2). Because of autocorrelation between many indices, this is not surprising. Considering that many researchers may prefer to stick with a univariate approach, but expand possible indices for consideration, I examined all indices significant at the 0.01 level with correlations >|0.30|.

The strongest correlate ($\rho = 0.393$) with the summary decline metric is the structure-insensitive pigment index (SIPI) developed by Peñuelas, Baret, and Filella (1995). SIPI is

Table 2. Spearman's Rho correlations between field-measured summary decline ratings and a suite of vegetation indices.

Traditional indices	Spearman's p	Index formula	Reference
AI	0.0758	B3/B1	Wolter and Townsend (2011)
DVI	−0.1541	[B4]-[B3]	Jordan (1969)
EVI	−0.215**	2.5 × (([B4]-[B3])/([B4] + (6 × [B3])-(7.5 × [B1]) + 1))	Huete et al. (2002)
GI	−0.1453	[B2]/[B3]	Sivanpillai et al. (2006)
MIR	−0.2343***	B5/B7	Elvidge and Lyon (1985)
MSAVI	−0.1541	0.5 × (2 × [B4] + 1-(Sqr(((2 × [B4] + 1) × (2 × [B4] + 1)))-(8 × ([B4]-[B3]))))	Qi et al. (1994)
MSI	0.3323***	B5/B4	Rock et al. (1986)
NDII 5	−0.3214***	(B4-B5)/(B4 + B5)	Hardisky, Klemas, and Smart (1983)
NDII 7	−0.2788***	(B4-B7)/(B4 + B7)	Hunt and Rock (1989)
NDVI	−0.1911**	([B4]-[B3])/([B4] + [B3])	Rouse et al. (1974)
OSAVI	−0.1993**	([B4]-[B3])/([B4] + [B3] + 0.16)	Rondeaux, Steven, and Baret (1996)
RAI	−0.2891***	B4/(B3 + B5)	Arzani and King (1997)
RDVI	−0.1921**	Sqr((([B4]-[B3])/([B4] + [B3])) × ([B4]-[B3])))	Roujean and Breon (1995)
RVI	−0.0307	[B4]/[B3]	Pearson and Miller (1972)
SARVI	0.1486	1.5 × (([B4]-([B3]-([B1]-[B3])))/([B4]-([B3] + ([B1]-[B3]) + 0.5)))	Huete, Justice, and Liu (1994)
SAVI	−0.1763*	1.5 × (([B4]-[B3])/([B4] + [B3] + 0.5))	Huete (1988)

		Index formula		
Narrowband indices	Spearman's p	Narrowband	Broadband equivalent	Reference
Aoki	**0.0286**	R_{550}/R_{800}	***B2/B4***	**Aoki, Yabuki, and Totsuka (1981)**
BNa	−0.1429	R_{800}-R_{550}	[B3]/[B2]	Buschman and Nagel (1993)
CMS	0.1911**	R_{694}/R_{760}	B3/B4	Carter (1994)
CSe	0.3237**	R_{694}/R_{420}	B3/B1	Carter (1994)

(*Continued*)

Table 2. (Continued).

Narrowband indices	Spearman's p	Index formula: Narrowband	Index formula: Broadband equivalent	Reference
Datt	0.0584	$R_{672} \times (R_{550} \times R_{708})$	[B3] × ([B2] × [B3])	Datt (1998)
Dattb	0.0938	R_{750}/R_{550}	[B3]/[B2]	Datt (1998)
Flo	**−0.2343****	$\boldsymbol{FD_{690}/FD_{735}}$	**([B4]-[B2])/([B5]-[B3])**	**Mohammed, Binder, and Gillies (1995)**
Gitc	−0.0057	$1/R_{700}$	1/B3	Gitelson, Merzlyak, and Chivkunova (2001)
GM	0.1606	R_{750}/R_{550}	[B4]/[B2]	Gitelson and Merzlyak (1994)
MCARI1	0.1806*	$1.2 \times ((2.5 \times (R_{800}\text{-}R_{670}))\text{-}(1.3 \times (R_{800}\text{-}R_{550})))$	1.2 × ((2.5 × ([B3]))-(1.3 × ([B4]-[B2])))	Haboudane et al. (2004)
MCARI2	**−0.2604*****	$\boldsymbol{1.5 \times ((2.5 \times (R_{800}\text{-}R_{670}))\text{-}(1.3 \times (R_{800}\text{-}R_{550})))/(Sqr((((2 \times R_{800}+1) \times (2 \times R_{800}+1))))\text{-}(6 \times R_{800}\text{-}(5 \times (Sqr(R_{670})))\text{-}0.5)))}$	1.5 × ((2.5 × ([B4]-[B3]))-(1.3 × ([B4]-[B2])))/(Sqr((((2 × [B4] + 1) × (2 × [B4] + 1))))-(6 × [B4]-(5 × (Sqr([B3])))-0.5)))	**Haboudane et al. (2004)**
MND705	−0.1166	$(R_{750}\text{-}R_{705})/(R_{750} + RR_{705} + 2R_{445})$	([B4]-B3)/(B4 + B3 + (2 × B1))	Sims and Gamon (2002)
MSR	−0.0307	$((R_{800}/R_{678})\text{-}1)/(Sqr((R_{800}/R_{670}) + 1))$	(([B4]/[B3])-1)/(Sqr([B4]/[B3]) + 1))	Chen (1996)
MSR705	0.0407	$(R_{750}\text{-}R_{445})/(R_{705}\text{-}R_{445})$	([B4]-[B1])/([B4] + [B1])	Sims and Gamon (2002)
MTVI	−0.1698*	$1.2 \times ((1.2 \times (R_{800}\text{-}R_{550}))\text{-}(2.5 \times (R_{670}\text{-}R_{550})))$	1.2 × ((1.2 × ([B4]-[B2]))-(2.5 × ([B3]-[B2])))	Haboudane et al. (2004)
MTVI2	−0.2853***	$(1.5 \times ((1.2 \times ([R_{800}]\text{-}[R_{550}]))\text{-}(2.5 \times ([R_{670}]\text{-}[R_{550}])))))/(Sqr(((2 \times [R_{800}] + 1) \times (2 \times [R_{800}] + 1))\text{-}(6 \times [R_{800}]\text{-}(5 \times (Sqr([R_{670}])))\text{-}0.5))$	(1.5 × ((1.2 × ([B4]-[B2]))-(2.5 × ([B3]-[B2])))))/(Sqr(((2 × [B4] + 1) × (2 × [B4] + 1))-(6 × [B4]-(5 × (Sqr([B3])))-0.5))	Haboudane et al. (2004)
NPCI	0.2837***	$(R_{680}\text{-}R_{430})/(R_{680} \times R_{430})$	(B3-B1)/(B3 + B1)	Peñuelas et al. (1994)
PSSRa	−0.0307	R_{600}/R_{680}	[B4]/[B3]	Blackburn (1998)
SIPI	**0.393*****	$\boldsymbol{(R_{803}\text{-}R_{445})/(R_{800}\text{-}R_{680})}$	**([B4]-[B1])/([B4]-[B3])**	**Peñuelas, Baret, and Filella (1995)**
SRPI	−0.2426**	R_{430}/R_{680}	[B1]/[B3]	Peñuelas et al. (1993)
TVI	−0.1654*	$0.5 \times (120 \times (R_{avg760\ to\ 800}\text{-}R_{avg530\ to\ 570}) - (200 \times (R_{avg650\ to\ 680}\text{-}R_{avg530\ to\ 570})$	0.5 × (120 × ([B4]-[B2])-200 × ([B3]-[B2]))	Broge and Leblanc (2001)
VogB	−0.2544***	FD_{715}/FD_{705}	([B4]-[B3])/([B5]-[B4])	Vogelmann, Rock, and Moss (1993)

Notes: *indicates $p < 0.1$,**$p < 0.05$ and ***$p < 0.01$. R denotes reflectance at the specified wavelength, FD denotes the first derivative centered at the specified wavelength, and B denotes the specified Landsat-5 (TM) band.
Variables in bold were selected for the final multivariate model.

based on a ratio between normalized reflectance at 450 nm where both carotenoids and chlorophylls demonstrate strong absorbance, and reflectance at 680 nm where only chlorophylls absorb. SIPI characterizes the proportion of total photosynthetic pigments to chlorophyll pigments (Peñuelas, Baret, and Filella 1995). Because vegetation stress typically manifests as reductions in photosynthetic pigments, changes in the ratio between pigment types have been successfully used to characterize early decline symptoms in vegetation (Peñuelas et al. 1994).

The strongest broadband-derived index correlate with the summary decline metric was the moisture stress index (MSI, $\rho = 0.332$) (Rock et al. 1986). A simple ratio of bands 5 and 4, this index makes use of repressed reflectance due to water absorbance in band 5, in combination with the water-insensitive NIR band. MSI has been significantly correlated with measured water content in multiple species (Cho and Skidmore 2006; Hunt and Rock 1989; Harris, Bryant, and Baird 2006). In 2007 there were no documented periods of abnormally dry conditions across the study area (five growing season weeks in abnormal status). However, water availability is a common stress agent in the Catskills, due to extensive areas of steep terrain and rocky, shallow soils.

Another broadband index significantly associated with the summary decline rating was the normalized difference infrared index (NDII5, $\rho = -0.321$; Hardisky, Klemas, and Smart 1983). Also based on the water-sensitive band 5, NDII5 increases with increasing canopy water content and has been associated with vegetation water content (Hardisky, Klemas, and Smart 1983) and water stress detection in agricultural crops (Jackson et al. 2004). In contrast, Hunt and Rock (1989) concluded that indices derived from near infrared and mid-infrared reflectance were not sensitive enough to remotely sense water stress. Because equivalent water thickness is correlated with leaf area index, water-sensitive indices such as NDII5 are also a proxy for leaf area and canopy density assessments (Hunt and Rock 1989). In this way NDII5 has also been used for forest canopy monitoring, including timber extraction intensity (Souza, Roberts, and Cochrane 2005) and post-hurricane forest damage (Wang et al. 2010).

Much of Carter's work has focused on identifying key narrowband indices for both vegetation stress detection and estimation of various pigment concentrations (Carter 1994; Carter, Cibula, and Miller 1996; Carter and Knapp 2001; Carter and Miller 1994; Carter and Spiering 2002). Although designed using narrowband field and laboratory sensors, one of the indices that he developed for early stress detection was also a significant correlate with the summary decline value ($\rho = 0.3237$) (Carter 1994) in its broadband form. Referred to here as Carter Stress ratio e (CS_e), this simple ratio is based on the relatively strong vegetation stress response at R_{694}, in conjunction with the relatively insensitive R_{420}. CS_e has been used to successfully differentiate stressed from non-stressed vegetation across various vegetation species and stress agents (Carter 1993, 1994). This consistent reflectance response has been attributed to stress-induced inhibition of chlorophyll production (Carter 1993). It has also been identified as a potential index for early stress detection, with early and consistent index response to induced stress in soybeans from day two of treatment until canopies collapsed at day seven (Carter and Miller 1994).

3.2. *Decline predictive model*

Considering that the field-measured summary decline rating incorporates multiple stress characteristics, I hypothesized that a combination of indices, sensitive to different vegetation parameters, may prove more accurate than any single index, even when controlling for the larger number of variables in the model. Using the 2007 field measurements for

Table 3. The final multivariate decline equation included five terms calibrated using Landsat-5 (TM) imagery over the Catskills, NY. Predictor variables each contribute unique information related to biophysical characteristics of vegetation stress.

Term	Paremeter estimate	Absorbance feature	Reference
Intercept	−51.763		
B5	0.946	Canopy moisture content, leaf area index, and total biomass	Vieira et al. (2003)
Aoki	0.706	Chlorophyll content	Aoki, Yabuki, and Totsuka (1981)
MCARI2 (modified chlorophyll absorption ratio)	−0.236	Green leaf area index	Haboudane et al. (2004)
SIPI (structural independent pigment index)	54.536	Carotenoids: chlorophyll	Peñuelas, Baret, and Filella (1995)
Flo (chlorophyll fluoresence index)	0.451	Chlorophyll fluoresence	Mohammed, Binder, and Gillies (1995)

calibration, I used a mixed, stepwise linear regression to identify the best fit predictive model. The resulting five-term model is based on a combination of narrowband-derived indices and Landsat-5 (TM) reflectance band 5 (Table 3). Each of these variables are sensitive to unique decline symptoms, including chlorophyll content, ratio of chlorophyll to carotenoids, canopy density, moisture content, and chlorophyll fluorescence. Because each predictor variable is associated with unique, stress-related biophysical characteristics, correlation between variables was negligible (maximum model VIF = 3.9).

Across 11 distinct forest types, the resulting equation was able to predict the continuous 0–10 summary decline rating with r^2 = 0.621, RMSE = 0.403, and jack-knifed PRESS RMSE = 0.436 (Figure 2). For comparison to more traditional categorical assessments, the 0–10 continuous summary decline rating was rounded to the nearest integer to assess accuracy for a 10-class scale, resulting in 65% accuracy. A coarser class comparison was conducted by including predictions within 1-class of the correct category in the accuracy count. This 'within one' approach resulted in 100% accuracy, indicating that

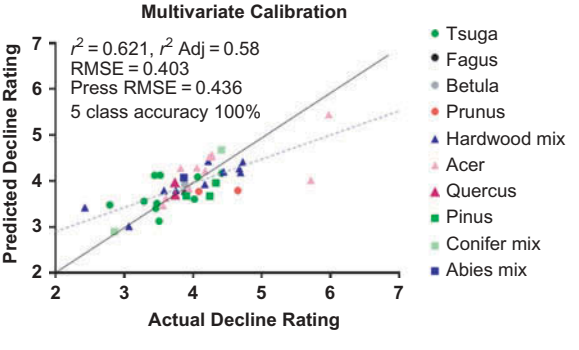

Figure 2. The final 5-term model was able to predict the 0–10 continuous summary decline rating with greater accuracy than traditional indices. While this equation holds across species, there is a tendency for plots at the extreme ends of the scale (highly productive and in severe decline) to be under- and over-predicted, respectively.

errors involved in model prediction are typically minor and do not exceed what would be necessary to accurately assign coarse categories of forest condition.

The benefit of a multivariate model is that where one index may not be able to successfully differentiate stand condition at a particular end of the decline range, a second variable may add accuracy for those decline conditions. For example, a means comparison of our final model indices indicates that while useful to characterize stands in the later stages of decline, SIPI cannot differentiate stands in pre-visual (class 3 mean = 1.001) and early decline (class 4 mean = 1.004). However, MCARI2 is able to differentiate class 3 (mean = 2.85) and class 4 (mean = 1.24) stands. Generally, healthy stands have relatively high values for Landsat TM Band 5 and MCARI2, with relatively lower values for Aoki and SIPI.

Allowing for the use of several indices is logical considering the variety of stress characteristics included in the summary decline rating used for calibration. One would expect that different indices may capture different physiological characteristics (e.g. chlorophyll content, canopy water content, chlorophyll fluorescence), each pertinent to the various field measures included in the calibration. But the danger is in over-fitting calibration data with each additional term added to the model. While building a complex model may create more appealing calibration fit statistics, there is a danger that accuracy is inflated with the inclusion of additional parameters. In addition to the regression diagnostics used during equation calibration (VIF and AIC), jack-knifed residuals and adjusted r^2 values were used to evaluate the possibility of over-fitting using the multivariate approach. When PRESS RMSE is close to full model RMSE, the predictive equation is considered to be stable (Kozak and Kozak 2003). At 0.436 and 0.403 the PRESS RMSE and RMSE are very similar, indicating that this model is robust and not simply fit to the data. In addition, an adjusted $r^2 = 0.57$ is a negligible reduction from the 0.62 reported for the full model. Even when considering only the adjusted r^2, the multivariate approach still outperforms traditional indices such as NDVI (see 3.3 below). Because of this suite of regression diagnostics (including the VIF and AIC considered in model development), I am confident that the reported accuracy of this model is not simply a result of the sample size, number of regressors, or autocorrelation among variables.

Several of the indices retained in the final predictive model are narrowband-derived indices designed to quantify various photosynthetic pigments. When plants are subjected to stress, many physiological changes occur, including: reduction in photosynthetic activity (Carter and Knapp 2001), inhibition of chlorophyll formation (Bourque and Naylor 1971), and an increasing breakdown of the chlorophyll molecule (Johnson 1988). Even subtle changes in these biophysical characteristics can alter reflectance patterns in the visible and near-infrared wavelengths (Carter and Knapp 2001; Gitelson and Merzlyak 1996; Vogelmann and Rock 1988; Vogelmann, Rock, and Moss 1993).

As the strongest global correlate discussed above, SIPI specifically targets the proportion of total photosynthetic pigments to chlorophyll pigments (Peñuelas, Baret, and Filella 1995). The ratio between these pigment types has been used specifically to identify early decline symptoms using narrowband imagery (Peñuelas et al. 1994). The modification for broadband calculation (Table 2) is based on the commonly used stress-sensitive Landsat-5 (TM) B3 and B4. However, it is the only index in the final model that makes use of Landsat-5 (TM) B1. While reflectance at this shorter wavelength helps distinguish between absorption by chlorophyll molecules and carotenoids, it is usually not considered in terrestrial vegetation studies because of the high levels of Rayleigh scatter and atmospheric interference. The strong correlation between SIPI and the summary decline index

tells us that the image pre-processing and atmospheric correction completed as a part of this study is sufficient to minimize this potential interference across image area and image acquisition dates.

A fluorescence index (Flo) was also retained in the final predictive model. Chlorophyll fluorescence can be used as an indirect measure of reductions in chlorophyll structure and function that typically occur in the earliest stages of vegetation stress (Strasser, Srivastava, and Govindjee 1995; Strasser and Tsimilli-Michael 2001). In field calibration measurements, I used a chlorophyll fluorescence meter to quantify this early stress symptom as the performance index (PI). PI is an estimate of how efficiently a leaf can absorb and use light while performing photosynthesis by quantifying the fluorescence response of leaves (Strasser and Tsimilli-Michael 2001). Such chlorophyll fluorescence metrics are shown to be an efficient tool to detect disturbances and damage to photosynthetic apparatus and function (Lichtenthaler 1992).

To capture the chlorophyll fluorescence response using reflectance spectra, Mohammed, Binder, and Gillies (1995) designed a narrowband ratio between first derivatives at F_{690} and F_{735} nm (Flo). Similar combinations of narrowband wavelengths in these regions have been used to quantify fluorescence (Lichtenthaler and Babani 2000; Buschmann and Lichtenthaler 1999; Gitelson, Buschmann, and Lichtenthaler 1999; Lichtenthaler et al. 1998; D'Ambrosio, Szabo, and Lichtenthaler 1992; Hak, Lichtenthaler, and Rinderle 1990; Rinderle and Lichtenthaler 1988). Regardless of the differences in specific narrowband location, each of these proposed fluorescence metrics can be modified for broadband calculation as Landsat-5 (TM) (B4-B2)/(B5-B3) (Table 2). Because of the direct measurement of fluorescence in the field calibration data, it is not surprising that a chlorophyll fluorescence index was retained in the final predictive model. It is likely that this index contributes predictive power at the low end of the summary decline rating, where reductions in chlorophyll structure and function are the dominant stress symptoms.

Based on a simple ratio between narrowband reflectance at 550 and 800 nm, the Aoki index (Aoki, Yabuki, and Totsuka 1981) was designed as a non-destructive method for estimating leaf chlorophyll concentration in multiple agricultural species. Blackburn and Steele (1999) also linked the Aoki index to total chlorophyll concentration in a laboratory study of deciduous leaves. However, they found an exponential relationship, indicating that the index may become insensitive at high chlorophyll concentrations. Saturation of the Aoki index would be expected at the low end of the decline rating scale. Considering this potential insensitivity to early decline, it is therefore not surprising that Aoki was not found to be a significant linear correlate with the summary decline rating. But as a predictor in a multivariate model, Aoki may contribute significantly to differentiating the more severe decline symptoms to which the other predictor variables (SIPI and Flo) are not as sensitive.

Similarly, MCARI2 is an index more sensitive to later symptoms of decline such as defoliation and canopy thinning through estimation of green leaf area index (LAI). Developed by Haboudane et al. (2004), MCARI2 is a modified variant of a spectral index originally intended to measure photosynthetically active radiation related to chlorophyll absorption. The goal of this modification was to create an index less sensitive to chlorophyll effects, more responsive to green LAI variations, and more resistant to soil and atmosphere effects (Haboudane et al. 2004). MCARI2 demonstrates a clear linear relationship with leaf area index, without a pronounced change of the slope or saturation at higher chlorophyll concentrations (Wu et al. 2010). Because reductions in leaf area index are most noticeable when decline includes more severe levels of dieback,

senescence, and general canopy thinning, it is likely that the MCARI2 index is providing information pertinent to distinguishing stands in more advanced stages of decline.

Water-sensitive bands provide insight to a stress characteristic that, while not directly measured in the field calibration data, provide an indirect assessment of canopy condition. Because many of the stress agents in the region, such as seasonal drought and heat stress, result in loss of turgor pressure, while other stressors such as hemlock woolly adelgid and beech bark disease impede stomatal conductance of water from roots to leaves, it is not surprising that a water-sensitive spectral region is included in the final model. Stress related to leaf water content is picked up in the mid-IR from 1400 to 2500 nm (covered in part by Landsat-5 (TM) band 5 at 1550 to 1750 nm) due to severe leaf dehydration and the accompanying decreased absorption by water (Carter 1993; Hunt and Rock 1989; Jensen 1996). There are several indices that make use of the spectral region covered by band 5 for canopy water content assessments. However, in the final stepwise regression model this single band provided a stronger, unique contribution to decline assessment than more complex moisture-sensitive indices based on multiple bands. Aside from its sensitivity to canopy moisture, other studies have also used Landsat-5 (TM) band 5 to assess forest biomass, species diversity, tree size, density, and leaf area index in tropical forests (Vieira et al. 2003).

3.3. *Model comparison to traditional indices*

In order to quantify how the multivariate model compares to the more common approach of utilizing individual indices, calibrations were also completed for several of the most common traditional broadband indices. The most accurate broadband index was NDVI (r^2 = 0.351, RMSE = 0.501). This is a notable departure from the accuracy obtained using the multivariate model discussed above (r^2 = 0.621, RMSE = 0.403). However, it is important to consider that NDVI is typically used to assign broad classes of canopy condition, as opposed to a continuous decline rating. NDVI accuracy as a class variable (10-class = 60%, 5-class = 74% accuracy) is consistent with previous studies utilizing Landsat to categorize forest decline (Lambert et al. 1995; Royle and Lathrop 2002; Wang, Lu, and Haithcoat 2007; Arsenault et al. 2006), with 75%, 82%, 76%, and 70% accuracy respectively. Treated as a class variable, the multivariate model proposed here is more accurate (10-class = 65%, 5-class = 100% accuracy) than any previous efforts using NDVI alone.

It is likely that NDVI does not predict the summary decline rating as well as the multivariate model, because of the inclusion of very early decline symptoms (fluorescence) in field calibration measurements. NDVI is known to saturate in dense canopies (Wang et al. 2010) and may not be able to distinguish the early stress response of decreased photosynthetic function that occurs in canopies that are still relatively dense. It is also possible that the inherent difference in NDVI across species confounds the stress signal within any given species.

To examine how multivariate output differs from traditional multispectral assessments across a landscape, I applied both the NDVI and multivariate calibrations to all pixels in the study region (Figure 3). While both NDVI and the multivariate model identify ‘hot spots’ of severe forest decline, the broader assessment of regional canopy condition and detail contained therein differ markedly between the two. Based on field data, NDVI over-predicted all plots in the 0–3 decline summary range, essentially lumping healthy stands with those in early decline. This is evident in the NDVI-predicted decline coverage (Figure 3), with less detail and differentiation between

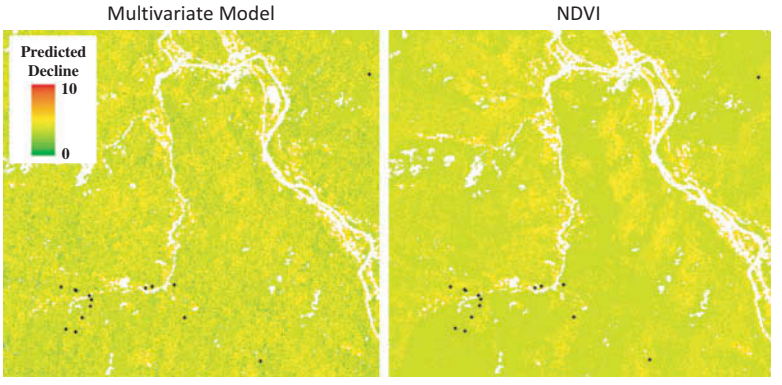

Figure 3. A comparison of the multivariate and NDVI predictions of forest condition at Woodland Valley (~UTM WGS84 556300 E 4656000 N), a region of severe hemlock woolly adelgid infestation. While both models detect similar locations of more severe decline, NDVI is not able to discriminate between healthy canopies from those in the early stages of decline. As a result, the NDVI assessment of the region suggests higher average decline condition across the region than the multivariate model and field measurements.

pixels than the multivariate model. This is probably a result of the tendency of NDVI to saturate at very high canopy density values (Wang et al. 2010). While this limits the ability of NDVI to monitor subtle changes in forest condition, it also alters the overall assessment of canopy conditions across the landscape. For the Catskills study area, the average predicted summary decline rating for the multivariate model was 3.97, compared with NDVI's 5.12. The field-measured average for the region was 3.93. This indicates that a regional analysis using NDVI would potentially overestimate decline conditions.

If the goal is to identify only stands in moderate to severe decline, this may not be of concern. If, however, the goal is to identify early stages of decline, such as those associated with incipient infestations by exotic pests and pathogens, the level of detail provided by the multivariate model would be critical.

It was outside of the scope of this work to compare additional calibration techniques. Instead, the focus was to investigate a suite of easily computed values that would be robust across species and stress agents for forest decline assessment. I recommend that future efforts to monitor forest decline consider this approach in order to maximize the information and accuracy possible with broadband sensors so widely available at this time.

4. Conclusions

The overarching goal of this study was to determine whether more detailed and accurate assessments of canopy condition can be achieved using the commonly available multispectral imagery. This approach was unique in several ways: (1) the use of a detailed, continuous summary decline rating for ground truth and model calibration; (2) consideration of narrowband-derived vegetation indices adapted for broadband data; and (3) calibration with a multivariate model designed to capture a range of decline symptoms. I found that forest condition could more accurately and consistently be predicted using a multivariate predictive model that includes consideration of narrowband derived indices.

The final 5-term linear regression model is based on existing narrowband-derived vegetation indices known for their sensitivity to chlorophyll structure and function, canopy density, and moisture content. To my knowledge, these narrowband indices have never been modified for multispectral application because of a widespread assumption that absorbance features targeted by the narrowband wavelength combinations are not detectable in the broadband imagery. While it is true that the original narrowband indices are likely to more accurately quantify the specific biophysical parameters for which they were designed, these results indicate that when calculated using broadband data, information relative to canopy condition is retained in spite of a loss of spectral resolution.

References

Adams, M. L., W. A. Norvell, W. D. Philpot, and J. H. Peverly. 2000. "Spectral Detection of Micronutrient Deficiency in 'Bragg' Soybean." *Agronomy Journal* 92 (2): 261–268. doi:10.1007/s100870050031.

Akaike, H. 1976. "An Information Criterion." *Math Science* 1: 5–9.

Aoki, M., K. Yabuki, and T. Totsuka. 1981. "An Evaluation of Chlorophyll Content of Leaves Based on the Spectral Reflectivity in Several Plants." *Research Report of the National Institute of Environmental Studies of Japan* 66: 125–130.

Arsenault, E. J., R. J. Hall, R. S. Skakun, E. H. Hogg, and M. Michaelian. 2006. "Characterizing Aspen Dieback and Severity Using Multidate Landsat Data in Western Canadian Forests." Paper presented at the Eleventh Forest Service Remote Sensing Applications Conference, Salt Lake City, UT, April 24–28.

Arzani, H., and G. W. King. 1997. "Application of Remote Sensing (Landsat TM Data) for Vegetation Parameters Measurement in Western Division of NSW." International Grassland Congress, Hohhot, June 29–July 5.

Blackburn, G. A. 1998. "Quantifying Chlorophylls and Caroteniods at Leaf and Canopy Scales: An Evaluation of Some Hyperspectral Approaches." *Remote Sensing of Environment* 66 (3): 273–285. doi:10.1016/S0034-4257(98)00059-5.

Blackburn, G. A., and C. M. Steele. 1999. "Towards the Remote Sensing of Matorral Vegetation Physiology: Relationships between Spectral Reflectance, Pigment, and Biophysical Characteristics of Semiarid Bushland Canopies." *Remote Sensing of Environment* 70 (3): 278–292. doi:10.1016/S0034-4257(99)00044-9.

Bourque, D. P., and A. W. Naylor. 1971. "Large Effects of Small Water Deficits on Chlorophyll Accumulation and Ribonucleic Acid Synthesis in Etiolated Leaves of Jack Bean (Canavalia Ensiformis [L.] DC.)." *Plant Physiology* 47: 591–594. doi:10.1104/pp.47.4.591.

Broge, N. H., and E. Leblanc. 2001. "Comparing Prediction Power and Stability of Broadband and Hyperspectral Vegetation Indices for Estimation of Green Leaf Area Index and Canopy Chlorophyll Density." *Remote Sensing of Environment* 76 (2): 156–172. doi:10.1016/S0034-4257(00)00197-8.

Buschmann, C., and H. K. Lichtenthaler. 1999. "Contribution of Chlorophyll Fluorescence to the Reflectance of Leaves in Stressed Plants as Determined with the Viraf-Spectrometer." *Zeitschrift Fur Naturforschung C-A Journal of Biosciences* 54 (9–10): 849–855.

Buschmann, C., and E. Nagel. 1993. "In Vivo Spectroscopy and Internal Optics of Leaves as Basis for Remote Sensing of Vegetation." *International Journal of Remote Sensing* 14: 711–722. doi:10.1080/01431169308904370.

Carter, G. A. 1993. "Responses of Leaf Spectral Reflectance to Plant Stress." *American Journal of Botany* 80 (3): 239–243. doi:10.2307/2445346.

Carter, G. A. 1994. "Ratios of Leaf Reflectances in Narrow Wavebands as Indicators of Plant Stress." *International Journal of Remote Sensing* 15 (3): 697–703. doi:10.1080/01431169408954109.

Carter, G. A. 1998. "Reflectance Wavebands and Indices for Remote Estimation of Photosynthesis and Stomatal Conductance in Pine Canopies." *Remote Sensing of Environment* 63 (1): 61–72. doi:10.1016/S0034-4257(97)00110-7.

Carter, G. A., W. G. Cibula, and R. L. Miller. 1996. "Narrow-Band Reflectance Imagery Compared with Thermal Imagery for Early Detection of Plant Stress." *Journal of Plant Physiology* 148 (5): 515–522. doi:10.1016/S0176-1617(96)80070-8.

Carter, G. A., and A. K. Knapp. 2001. "Leaf Optical Properties in Higher Plants: Linking Spectral Characteristics to Stress and Chlorophyll Concentration." *American Journal of Botany* 88 (4): 677–684. doi:10.2307/2657068.

Carter, G. A., and R. L. Miller. 1994. "Early Detection of Plant Stress by Digital Imaging within Narrow Stress-Sensitive Wavebands." *Remote Sensing of Environment* 50 (3): 295–302. doi:10.1016/0034-4257(94)90079-5.

Carter, G. A., and B. A. Spiering. 2002. "Optical Properties of Intact Leaves for Estimating Chlorophyll Concentration." *Journal of Environment Quality* 31 (5): 1424–1432. doi:10.2134/jeq2002.1424.

Chander, G., B. L. Markham, and D. L. Helder. 2009. "Summary of Current Radiometric Calibration Coefficients for Landsat MSS, TM, ETM+, and EO-1 ALI Sensors." *Remote Sensing of Environment* 113 (5): 893–903. doi:10.1016/j.rse.2009.01.007.

Chavez, P. S. 1988. "An Improved Dark-Object Subtraction Technique for Atmospheric Scattering Correction of Multispectral Data." *Remote Sensing of Environment* 24: 459–479. doi:10.1016/0034-4257(88)90019-3.

Chen, J. 1996. "Evaluation of Vegetation Indices and a Modified Simple Ratio for Boreal Applications." *Canadian Journal of Remote Sensing* 22 (3): 229–242.

Cho, M. A., and A. K. Skidmore. 2006. "A New Technique for Extracting the Red Edge Position from Hyperspectral Data: The Linear Extrapolation Method." *Remote Sensing of Environment* 101: 181–193. doi:10.1016/j.rse.2005.12.011.

D'Ambrosio, N., K. Szabo, and H. K. Lichtenthaler. 1992. "Increase of the Chlorophyll Fluorescence Ratio F690/F735 during the Autumnal Chlorophyll Breakdown." *Radiation and Environmental Biophysics* 31 (1): 51–62. doi:10.1007/BF01211512.

Datt, B. 1998. "Remote Sensing of Chlorophyll A, Chlorophyll B, Chlorophyll A + B, and Total Carotenoid Content in Eucalyptus Leaves." *Remote Sensing of Environment* 66: 111–121. doi:10.1016/S0034-4257(98)00046-7.

Elvidge, C. D., and R. J. P. Lyon. 1985. "Estimation of the Vegetation Contribution to the 1.65/2.22 um Ratio in Airborne Thematic Mapper Imagery of the Virginia Range, Nevada." *International Journal of Remote Sensing* 6 (1): 75–88.

Gitelson, A. A., C. Buschmann, and H. K. Lichtenthaler. 1999. "The Chlorophyll Fluorescence Ratio F-735/F-700 as an Accurate Measure of the Chlorophyll Content in Plants." *Remote Sensing of Environment* 69 (3): 296–302. doi:10.1016/S0034-4257(99)00023-1.

Gitelson, A. A., and M. N. Merzlyak. 1994. "Quantitative Estimateion of Chlorophyll-A Using Reflectance SpectraZ: Experiments with Autumn Chestnut and Maple Leaves." *Journal of Photochemical Phyogbiology* 22: 247–252.

Gitelson, A. A., and M. N. Merzlyak. 1996. "Signature Analysis of Leaf Reflectance Spectra: Algorithm Development for Remote Sensing of Chlorophyll." *Journal of Plant Physiology* 148: 494–500. doi:10.1016/S0176-1617(96)80284-7.

Gitelson, A. A., M. N. Merzlyak, and O. B. Chivkunova. 2001. "Optical Properties and Nondestructive Estimation of Anthocyanin Content in Plant Leaves." *Photochemistry and Photobiology* 74 (1): 38–45. doi:10.1562/0031-8655(2001)074<0038:OPANEO>2.0.CO;2.

Haboudane, D., J. R. Miller, E. Pattey, P. J. Zarco-Tejada, and I. B. Strachan. 2004. "Hyperspectral Vegetation Indices and Novel Algorithms for Predicting Green LAI of Crop Canopies: Modeling and Validation in the Context of Precision Agriculture." *Remote Sensing of Environment* 90 (3): 337–352. doi:10.1016/j.rse.2003.12.013.

Hak, R., H. K. Lichtenthaler, and U. Rinderle. 1990. "Decrease of the Chlorophyll Fluorescence Ratio F690/F730 during Greening and Development of Leaves." *Radiation and Environmental Biophysics* 29 (4): 329–336. doi:10.1007/BF01210413.

Hardisky, M. A., V. Klemas, and R. M. Smart. 1983. "The Influence of Soil Salinity, Growth Form, and Leaf Moisture on the Spectral Radiance of Spartina Alterniflora Canopies." *Photogrammetric Engineering and Remote Sensing* 49 (1): 77–83.

Harris, A., R. G. Bryant, and A. J. Baird. 2006. "Mapping the Effects of Water Stress on Sphagnum: Preliminary Observations Using Airborne Remote Sensing." *Remote Sensing of Environment* 100: 363–378. doi:10.1016/j.rse.2005.10.024.

Huete, A., K. Didan, T. Miura, E. P. Rodriguez, X. Gao, and L. G. Ferreira. 2002. "Overview of the Radiometric and Biophysical Performance of the MODIS Vegetation indices." *Remote Sensing of Environment* 83 (1–2): 195–213.

Huete, A., C. Justice, and H. Liu. 1994. "Development of Vegetation and Soil Indices for MODIS-EOS." *Remote Sensing of Environment* 49 (3): 224–234. doi:10.1016/0034-4257(94)90018-3.

Huete, A. R. 1988. "A Soil Adjusted Vegetation Index (SAVI)." *Remote Sensing of Environment* 25 (3): 295–309.

Hunt Jr., E. R., and B. N. Rock. 1989. "Detection of Changes in Leaf Water Content Using Near- and Middle-Infrared Reflectances." *Remote Sensing of Environment* 30 (1): 43–54. doi:10.1016/0034-4257(89)90046-1.

Jackson, T. L., D. Chen, M. Cosh, F. Li, M. Anderson, C. Walthall, P. Doriaswamy, and E. R. Hunt. 2004. "Vegetation Water Content Mapping Using Landsat Data Derived Normalized Difference Water Index for Corn and Soybeans." *Remote Sensing of Environment* 92: 475–482. doi:10.1016/j.rse.2003.10.021.

Jensen, J. R. 1996. *Introductory Digital Image Processing: A Remote Sensing Perspective*. Englewood Cliffs, NJ: Prentice-Hall.

Johnson, J. D. 1988. "Stress Physiology of Forest Trees: The Role of Plant Growth Regulators." In *Lant Growth Regulation*, 193–215. Dordrecht: Martinus Nijhoff.

Jordan, C. F. 1969. "Derivation of Leaf Area Index from Quality of Light on the Forest Floor." *Ecology (Washington, DC)* 50 (4): 663–666. doi:10.2307/1936256.

Keane, R. E., P. Morgan, and J. P. Menakis. 1994. "Landscape Assessment of the Decline of Whitebark Pine (Pinus Albicaulis) in the Bob Marshall Wilderness Complex, Montana, USA." *Northwest Science* 68 (3): 213–229.

Kleinbaum, D. G., L. L. Kupper, K. E. Muller, and A. Nizam. 1998. "Applied Regression Analysis and Other Multivariable Methods." In *Applied Regression Analysis and Other Multivariable Methods*, edited by D. G. Kleinbaum, L. L. Kupper, K. E. Muller, and A. Nizam, 314–319. Pacific Grove, CA: Cole Publishing Company.

Kozak, A., and R. Kozak. 2003. "Does Cross Validation Provide Additional Information in the Evaluation of Regression Models?" *Canadian Journal of Forest Research* 33: 976–987. doi:10.1139/x03-022.

Lambert, N. J., J. Ardo, B. N. Rock, and J. E. Vogelmann. 1995. "Spectral Characterization and Regression-Based Classification of Forest Damage in Norway Spruce Stands in the Czech-Republic Using Landsat Thematic Mapper Data." *International Journal of Remote Sensing* 16 (7): 1261–1287. doi:10.1080/01431169508954476.

Lichtenthaler, H. K. 1992. "The Kautsky Effect: 60 Years of Chlorophyll Fluorescence Induction Kinetics." *Photosynthetica* 27: 45–55.

Lichtenthaler, H. K., and F. Babani. 2000. "Detection of Photosynthetic Activity and Water Stress by Imaging the Red Chlorophyll Fluorescence." *Plant Physiology and Biochemistry* 38 (11): 889–895. doi:10.1016/S0981-9428(00)01199-2.

Lichtenthaler, H. K., O. Wenzel, C. Buschmann, and A. Gitelson. 1998. "Plant Stress Detection by Reflectance and Fluorescence." In *Stress of Life*, 271–285. New York: Annals of the New York Academy of Sciences.

Mohammed, G. H., W. D. Binder, and S. L. Gillies. 1995. "Chlorophyll Fluorescence: A Review of its Practical Forestry Applications and Instrumentation." *Scandinavian Journal of Forest Research* 10 (1–4): 383–410. doi:10.1080/02827589509382904.

Pearson, L., and L. D. Miller. 1972. "Remote Mapping of Standing Crop Biomass for Estimation of the Productivity of the Short-Grass Prairie, Pawnee National Grasslands, Colorado." Paper presented at the Proceedings of the 8th International Symposium on Remote Sensing of the Environment, Ann Arbor, MI, October 6–7.

Peñuelas, J., F. Baret, and I. Filella. 1995. "Semi-Empirical Indices to Assess Carotenoids/Chlorophyll a Ratio from Leaf Spectral Reflectance." *Photosynthetica* 31: 221–230.

Peñuelas, J., J. A. Gamon, A. L. Fredeen, J. Merino, and C. B. Field. 1994. "Reflectance Indices Associated with Physiological Changes in Nitrogen- and Water-Limited Sunflower Leaves." *Remote Sensing of Environment* 48 (2): 135–146. doi:10.1016/0034-4257(94)90136-8.

Peñuelas, J., J. A. Gamon, K. L. Griffin, and C. B. Field. 1993. "Assessing Community Type, Plant Biomass, Pigment Composition, and Photosynthetic Efficiency of Aquatic Vegetation from Spectral Reflectance." *Remote Sensing of Environment* 46 (2): 110–118. doi:10.1016/0034-4257(93)90088-F.

Pontius, J. and R. Hallett. 2014. "Comprehensive Methods for Earlier Detection and Monitoring of Forest Decline." *Forest Science*. doi:10.5849/forsci.13-121.

Pontius, J., R. Hallett, and M. Martin. 2005a. "Using AVIRIS to Assess Hemlock Abundance and Early Decline in the Catskills, New York." *Remote Sensing of Environment* 97: 163–173. doi:10.1016/j.rse.2005.04.011.

Pontius, J., R. Hallett, and M. Martin. 2005b. "Assessing Hemlock Decline Using Visible and Near-Infrared Spectroscopy: Indices Comparison and Algorithm Development." *Journal of Applied Spectroscopy* 59: 836–843. doi:10.1366/0003702054280595.

Pontius, J., M. Martin, L. Plourde, and R. Hallett. 2008. "Ash Decline Assessment in Emerald Ash Borer Infested Regions: A Test of Tree-Level, Hyperspectral Technologies." *Remote Sensing of Environment* 112 (5): 2665–2676. doi:10.1016/j.rse.2007.12.011.

Qi, J., A. Chehbouni, A. R. Huete, Y. H. Kerr, and S. Sorooshian. 1994. "A Modified Soil Adjusted Vegetation Index." *Remote Sensing of Environment* 48 (2): 119–126. doi:10.1016/0034-4257(94)90134-1.

Rinderle, U., and H. K. Lichtenthaler. 1988. "The Chlorophyll Fluorescence Ratio F690/F735 as a Possible Stress Indicator." In *Applications of Chlorophyll Fluorescence*, 176–183. Dordrecht: Kluwer Adademic Press.

Rock, B. N., A. F. Vogelmann, D. L. Williams, D. L. Vogelmann, and T. Hoshizaki. 1986. "Remote Detection of Forest Damage." *Bioscience* 36 (7): 439–445.

Rondeaux, G., M. Steven, and F. Baret. 1996. "Optimization of Soil-Adjusted Vegetation Indices." *Remote Sensing of Environment* 55 (2): 95–107. doi:10.1016/0034-4257(95)00186-7.

Roujean, J.-L., and F.-M. Breon. 1995. "Estimating PAR Absorbed by Vegetation from Bidirectional Reflectance Measurements." *Remote Sensing of Environment* 51 (3): 375–384. doi:10.1016/0034-4257(94)00114-3.

Rouse, J., R. Hass, J. Schell, D. Deering, and J. Harlan. 1974. "Monitoring the Vernal Advancement and Retrogradation of Natural Vegetation." In *NASA Report*. Greenbelt, MD: NASA.

Royle, D. D., and R. G. Lathrop. 2002. "Discriminating Tsuga Canadensis Hemlock Forest Defoliation Using Remotely Sensed Change Detection." *Journal of Nematology* 34 (3): 213–221.

Sims, D. A., and J. A. Gamon. 2002. "Relationships Between Leaf Pigment Content and Spectral Reflectance Across a Wide Range of Species, Leaf Structures and Developmental Stages." *Remote Sensing of Environment* 81 (2–3): 337–354.

Sivanpillai, R., C. T. Smith, R. Srinivasan, M. G. Messina, and X. B. Wu. 2006. "Estimation of Managed Loblolly Pine Stand Age and Density with Landsat ETM+ Data." *Forest Ecology and Management* 223 (1–3): 247–254. doi:10.1016/j.foreco.2005.11.013.

Song, C., C. E. Woodcock, K. C. Seto, M. P. Lenney, and S. A. Macomber. 2001. "Classification and Change Detection Using Landsat TM Data: When and How to Correct Atmospheric Effects?" *Remote Sensing of Environment* 75 (2): 230–244. doi:10.1016/S0034-4257(00)00169-3.

Soudani, K., C. François, G. le Maire, V. Le Dantec, and E. Dufrêne. 2006. "Comparative Analysis of IKONOS, SPOT, and ETM+ Data for Leaf Area Index Estimation in Temperate Coniferous and Deciduous Forest Stands." *Remote Sensing of Environment* 102 (1–2): 161–175. doi:10.1016/j.rse.2006.02.004.

Souza Jr., C. M., D. A. Roberts, and M. A. Cochrane. 2005. "Combining Spectral and Spatial Information to Map Canopy Damage from Selective Logging and Forest Fires." *Remote Sensing of Environment* 98: 329–343. doi:10.1016/j.rse.2005.07.013.

Strasser, R. J., A. Srivastava, and Govindjee. 1995. "Polyphasic Chlorophyll A Fluorescence Transient in Plants and Cyanobacteria." *Photochemistry and Photobiology* 61 (1): 32–42. doi:10.1111/j.1751-1097.1995.tb09240.x.

Strasser, R. J., and M. Tsimilli-Michael. 2001. "Stress in Plants, from Daily Rhythm to Global Changes, Detected and Quantified by the JIP-Test." *Chimie Nouvelle. Belgian Royal Society of Chemistry* 75: 3321–3326.

Townsend, P. A., A. Singh, J. R. Foster, N. J. Rehberg, C. C. Kingdon, K. N. Eshleman, and S. W. Seagle. 2012. "A General Landsat Model to Predict Canopy Defoliation in Broadleaf Deciduous Forests." *Remote Sensing of Environment* 119: 255–265. doi:10.1016/j.rse.2011.12.023.

USDA, Forest Service. 1997. *Forest Health Monitoring 1997 Field Methods Guide*. Research Triangle Park, NC: US Department of Agriculture, Forest Service, National Forest Health Monitoring Program.

Vieira, I. C. G., A. Silva de Almeida, E. R. Davidson, T. A. Stone, C. J. Reis de Carvalho, and J. B. Guerrero. 2003. "Classifying Successional Forests Using Landsat Spectral Properties and Ecological Characteristics in Eastern Amazônia." *Remote Sensing of Environment* 87: 470–481. doi:10.1016/j.rse.2002.09.002.

Vogelmann, J. E., and B. N. Rock. 1988. "Assessing Forest Damage in High-Elevation Coniferous Forests in Vermont and New-Hampshire Using Thematic Mapper Data." *Remote Sensing of Environment* 24 (2): 227–246. doi:10.1016/0034-4257(88)90027-2.

Vogelmann, J. E., B. N. Rock, and D. M. Moss. 1993. "Red Edge Spectral Measurements from Sugar Maple Leaves." *International Journal of Remote Sensing* 14 (8): 1563–1575. doi:10.1080/01431169308953986.

Wang, C., Z. Lu, and T. L. Haithcoat. 2007. "Using Landsat Images to Detect Oak Decline in the Mark Twain National Forest, Ozark Highlands." *Forest Ecology and Management* 240 (1–3): 70–78. doi:10.1016/j.foreco.2006.12.007.

Wang, W. T., J. J. Qu, X. J. Hao, Y. Q. Liu, and J. A. Stanturf. 2010. "Post-Hurricane Forest Damage Assessment Using Satellite Remote Sensing." *Agricultural and Forest Meteorology* 150 (1): 122–132. doi:10.1016/j.agrformet.2009.09.009.

Williams, P., and K. Norris. 2001. *Near-Infrared Technology in the Agricultural and Food Industries*. St. Paul, MN: American Association of Cereal Chemists.

Wolter, P. T., and P. A. Townsend. 2011. "Multi-Sensor Data Fusion for Estimating Forest Species Composition and Abundance in Northern Minnesota." *Remote Sensing of Environment* 115 (2): 671–691. doi:10.1016/j.rse.2010.10.010.

Wu, C., X. Han, Z. Niu, and J. Dong. 2010. "An Evaluation of EO-1 Hyperspectral Hyperion Data for Chlorophyll Content and Leaf Area Index Estimation." *International Journal of Remote Sensing* 31: 1079–1086. doi:10.1080/01431160903252335.